

Table S1. IC₅₀ of PTX-loaded PEG-FTS micelles compared to free PTX in 4T1.2 mouse breast cancer cell line.

IC ₅₀ (ng/mL)				
PTX	PEG _{2K} -FTS ₂ /PTX	PEG _{2K} -FTS ₄ /PTX	PEG _{5K} -FTS ₂ /PTX	PEG _{5K} -FTS ₄ /PTX
202.0	72.8	181.8	59.3	33.2

Figure legends

Figure S1. ¹H NMR spectra (400MHz) of PEG_{2K}-FTS₂ (A), PEG_{2K}-FTS₄ (B), PEG_{5K}-FTS₂ (C) and PEG_{5K}-FTS₄ (D) conjugates in CDCl₃.

Figure S2. MADLI-TOF of PEG_{2K}-FTS₂ (A), PEG_{2K}-FTS₄ (B), PEG_{5K}-FTS₂ (C) and PEG_{5K}-FTS₄ (D) conjugates.

Figure S3. The size distribution of free PEG_{2K}-FTS₂ (A), PEG_{2K}-FTS₄ (C), PEG_{5K}-FTS₂ (E) micelles and PTX-loaded PEG_{2K}-FTS₂ (B), PEG_{2K}-FTS₄ (D), PEG_{5K}-FTS₂ (F) micelles in PBS measured by dynamic light scattering (DLS).

Figure S4. Transmission electron microscopy (TEM) of free PEG_{2K}-FTS₂ (A), PEG_{2K}-FTS₄ (C), PEG_{5K}-FTS₂ (E) micelles and PTX-loaded PEG_{2K}-FTS₂ (B), PEG_{2K}-FTS₄ (D), PEG_{5K}-FTS₂ (F) micelles.

Figure S5. Critical micelle concentration (CMC) of PEG_{2K}-FTS₂ (A), PEG_{2K}-FTS₄ (B), PEG_{5K}-FTS₂ (C) and PEG_{5K}-FTS₄ (D) micelles.

Figure S1. ^1H NMR spectra (400MHz) of PEG_{2K}-FTS₂ (A), PEG_{2K}-FTS₄ (B), PEG_{5K}-FTS₂ (C) and PEG_{5K}-FTS₄ (D) conjugates in CDCl₃.

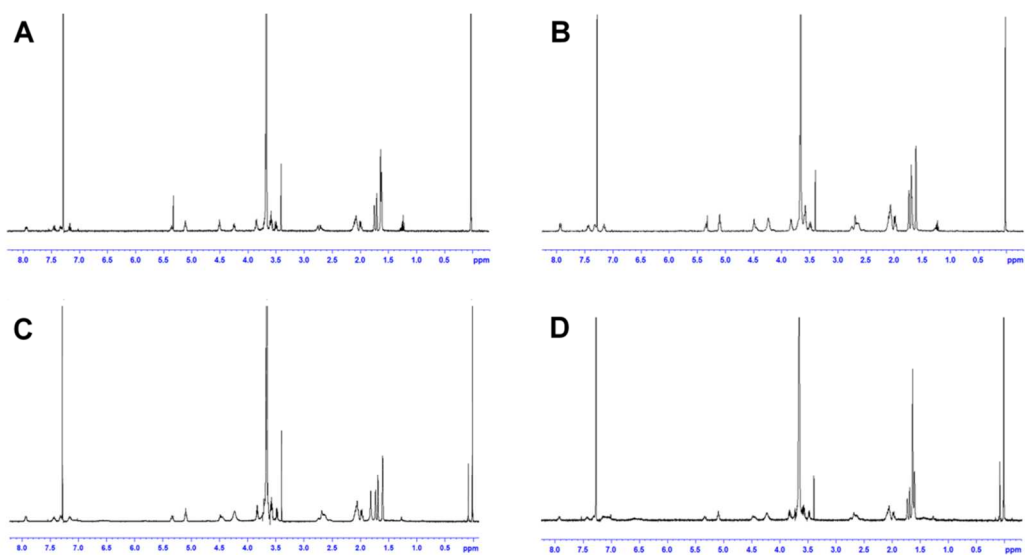


Figure S2. MADLI-TOF of PEG_{2K}-FTS₂ (A), PEG_{2K}-FTS₄ (B), PEG_{5K}-FTS₂ (C) and PEG_{5K}-FTS₄ (D) conjugates.

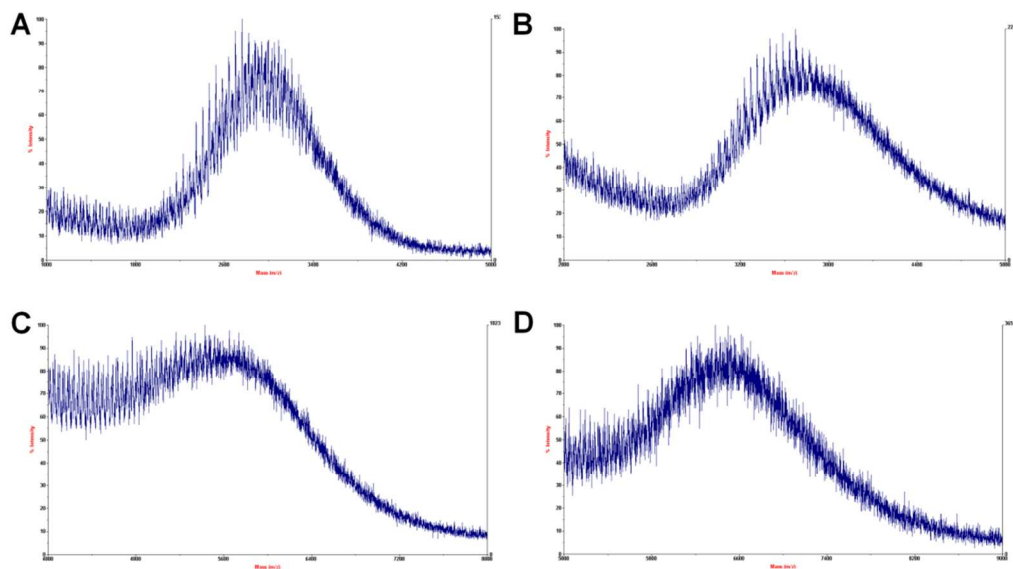


Figure S3. The size distribution of free PEG_{2K}-FTS₂ (A), PEG_{2K}-FTS₄ (C), PEG_{5K}-FTS₂ (E) micelles and PTX-loaded PEG_{2K}-FTS₂ (B), PEG_{2K}-FTS₄ (D), PEG_{5K}-FTS₂ (F) micelles in PBS measured by dynamic light scattering (DLS).

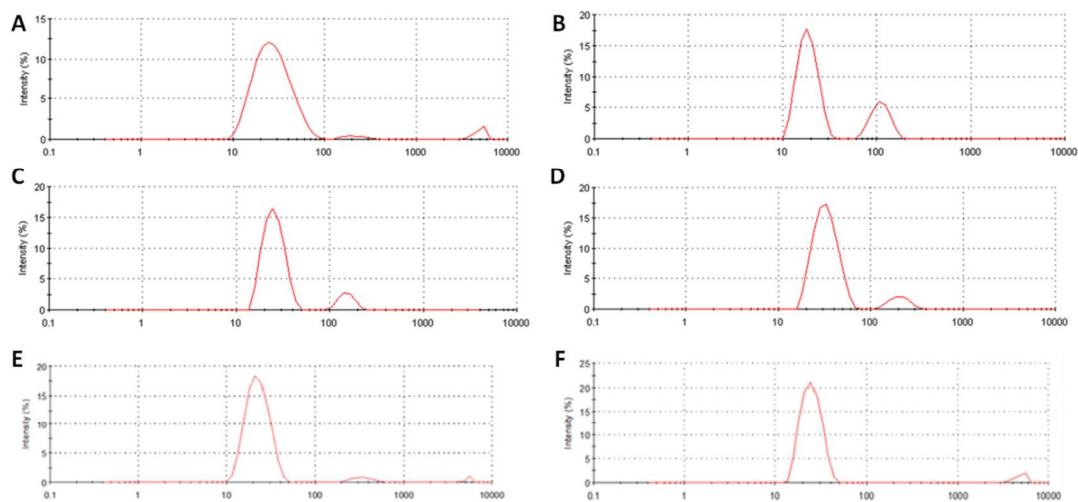


Figure S4. Transmission electron microscopy (TEM) of free PEG_{2K}-FTS₂ (A), PEG_{2K}-FTS₄ (C), PEG_{5K}-FTS₂ (E) micelles and PTX-loaded PEG_{2K}-FTS₂ (B), PEG_{2K}-FTS₄ (D), PEG_{5K}-FTS₂ (F) micelles.

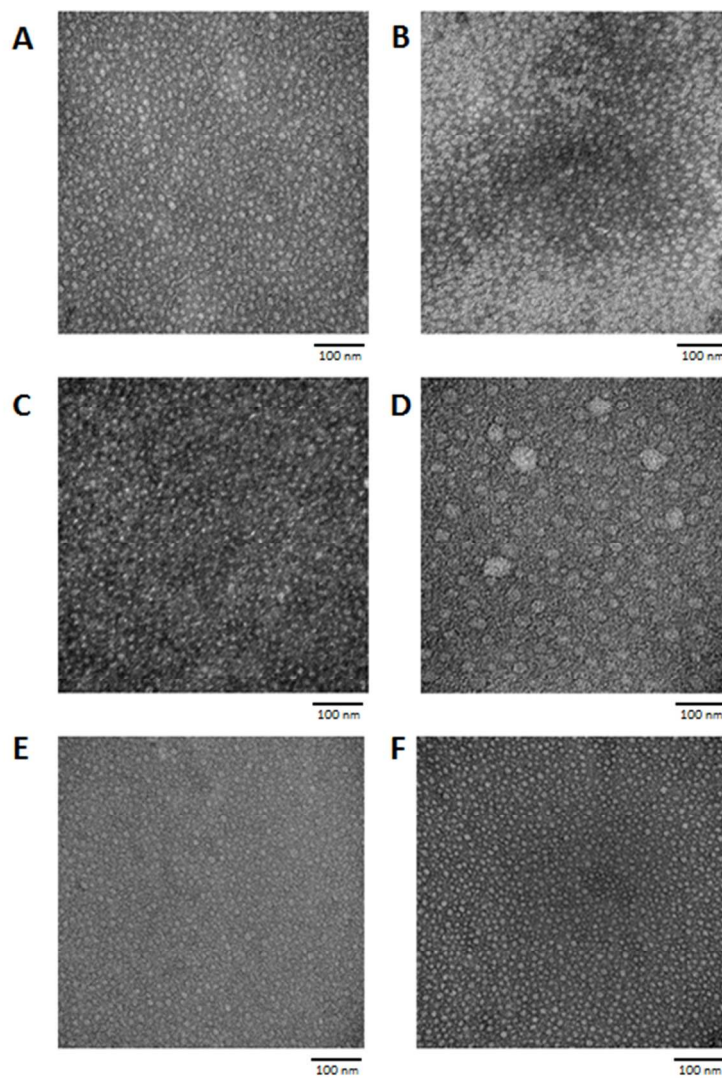


Figure S5. Critical micelle concentration (CMC) of PEG_{2K}-FTS₂ (A), PEG_{2K}-FTS₄ (B), PEG_{5K}-FTS₂ (C) and PEG_{5K}-FTS₄ (D) micelles.

